Proceedings of the 5th European International Conference on Industrial Engineering and Operations Management Rome, Italy, July 26-28, 2022

Multi-Optimization of Line Start Permanent Magnet Assistance Synchronous Reluctance Considering Skewed Effect and Demagnetization

[1]Bui Minh Dinh,

[1]Hanoi University of Science and Technology (HUST)
dinh.buiminh@hust.edu.vn
[2]Faculty of Electrical-Electronic Engineering
University of Transport and Communications (UTC)
tienan7876@gmail.com

Abstract

LS-PMA-SynRMs can operate with a direct start for net voltage or drive-by power converter with torque control methods. Especially, the LS-PMA-SynRM has a higher irreversible demagnetization level than IPM because it has a less permanent magnet in rotor slots in comparison with IPM. This paper will develop different rotor designs and modeling of a line-start permanent magnet assistance synchronous reluctance motor (LS-PMA-SynRM) with permanent magnets arrangement in V type considering skew slot and demagnetization effect. The short circuit current is analyzed and compared by finite element analysis FEA in no skewed and skew slots. The demagnetization performance of LS-PMA-SynRM is analyzed considering V magnet shape and skewed angle. The proposed model of LS-PMA-SynRM has been improved efficiency, torque, and output power. Finally, the LS-PMA-SynRM with 3V layered magnets rotor is prototyped to verify by full efficiency map to evaluate EVs application.

Keywords : LS-PMA-SynRM, Line Start-Permanent Magnet Assistance-Synchronous Reluctance (LS-PMA-SynRM), Fenite Element Analysis-FEA.

1. INTRODUCTION

Recent studies show that line start permanent magnet assistance synchronous reluctance (LS-PMA-SynRMs) present promising technologies because of their advantages such as simple structure and minimized the amount of permanent magnet Hyunwoo Kim 2020 and Cheng Gong 2021. Therefore, new types of motor are being studied to improve the efficiency of Line Start Permanent Magnet Assistance Synchronous Reluctance Motors (LS-PMA-SynRMs). When LS-PMA-SynRMs are operated at a synchronous speed, the secondary copper loss is eliminated so the efficiency can improve significantly. To save energy, use less rare-earth materials, and decrease the cost in terms of material and manufacturing processes LS-PMA-SynRMs are a good choice. A comprehensive study on line starts permanent magnet assistance synchronous reluctance (LS-PMA-SynRMs) is developed for direct start or torque control methods by power inverters. This study shows that the LS-PMA-SynRM has less rare-earth materials, low cost, comparable constant-power speed range, maximum torque per ampere, and efficiency of LS-PMa-SynRMs. In particular, LS-PMA-SynRMs have an interesting choice in electric traction and more-electrical aircraft applications because they have a special flux barrier and magnet arrangement to improve constant torque in wide range speed and less risk of irreversible demagnetization in short circuit and overheat temperature.

2. ELECTROMAGNETIC DESIGN OF LS- PMA-SYNRM

Electromagnetic design of LS-PMA-SynRM, 6-pole are designed as Figure 1. The stators of LS-PMa-SynRM have 36 slots, three types of rotor with 36 round bars. A magnetic material and silicon steels are N38UH and 35A350.

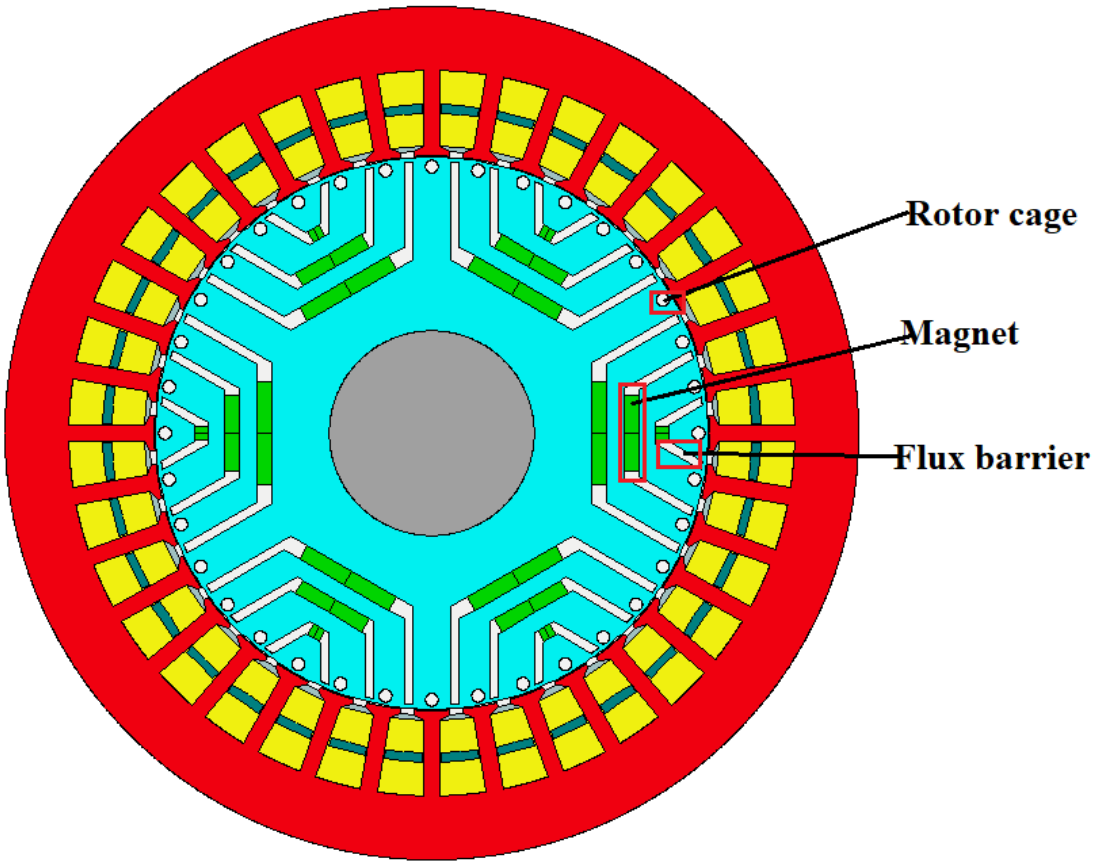

Figure 1. LS-PMA-SynRM with 3V Layer

The LS-PMA-SynRM-6P with 3 layers have been developed from IM 7500W-6P. The selected magnets in this motor are made of N38UH. This study is interested in the response of magnets to demagnetizing influence. Depending on the design specification, the machine may either need to withstand irreversible demagnetization during a transient short circuit fault condition or may only require that demagnetization is avoided during steady-state operating conditions. For sintered NdFeB and SmCo magnets, irreversible demagnetization is most likely to occur at high temperatures, i.e. above 120°C. For sintered Ferrite magnets, irreversible demagnetization is most likely to occur at low temperatures, i.e. below 0°C. The first step is to set the temperature at which you wish to investigate possible demagnetization. For this example, we will assume that the magnet temperature is 160°C.

In the magnet datasheet for your selected magnet (N38UH in this case), find the knee point of the magnet BH (demagnetization) curve at the specified magnet temperature. The knee joint is the flux density at which the BH curve becomes non-linear. If the flux density in the magnet is depressed below that point, there will be irreversible demagnetization in the magnet. In the plot below, the curve at 150°C becomes non-linear at about 0.2 T – at 160°C (the magnet temperature of our model), the knee point will be higher, indicating the magnet is more easily irreversibly demagnetized at high temperatures.

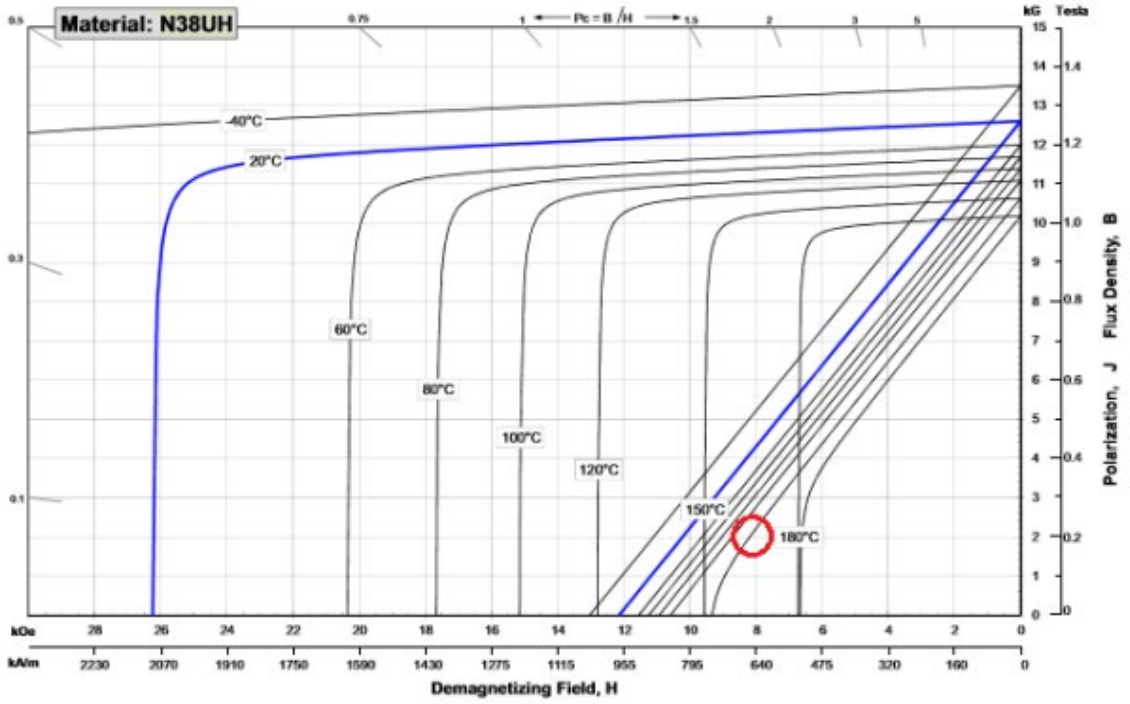

Figure 2 B-H Magnetization curve

FEM simulation generates non-linear demagnetization curves for magnets using magnet properties that are easily obtainable from magnet datasheets. It uses the model

$$B = Br + \mu_0\mu_r H - E \cdot e^{-k_1 \cdot (k_2 + H)},$$

$$k_2 = -\frac{ln\left[(Br + (\mu_r - 1) \cdot \mu_0 \cdot HcJ) \cdot \frac{1}{E}\right]}{k_1} - HcJ \quad (1)$$

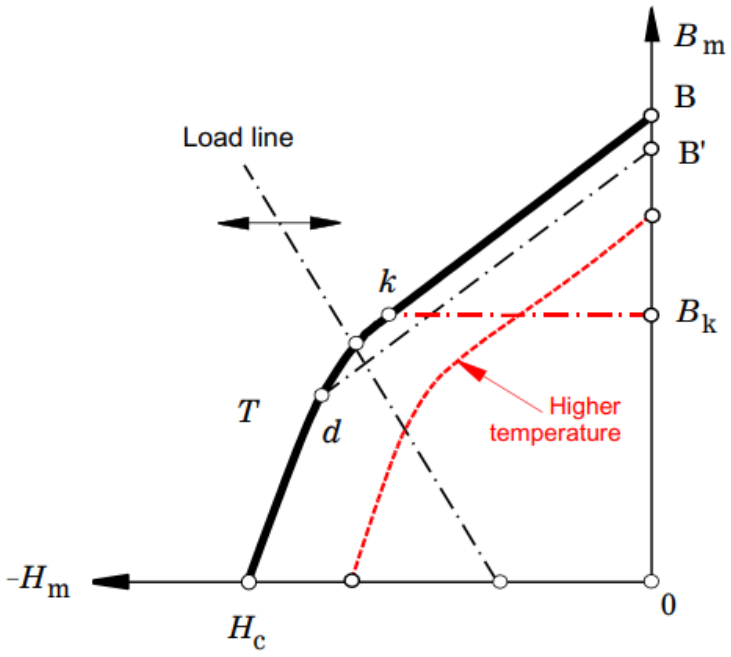

Figure 3 B-H Magnetization curve with higher temperature

In simple terms, the operating point of the magnet is defined by the flux-density Bm and the magnetic field strength Hm in the magnet. These define a point on the demagnetization characteristic which is at the intersection of the magnet characteristic and the load line. The slope of the load line is called the permeance coefficient, and it is determined principally by the ratio of the magnet length LM to the airgap g. When the machine is under load, the whole load line shifts, usually to the left, so the operating point is shifted further down the curve. Once it passes the knee, there will be an irreversible loss of magnetization. The objective in demagnetization calculations is to make sure that the magnet operating point stays above the knee. All points in the magnet cross-section might not all be the same. That's why we need the finite-element method. We also need to be sure that we are working with worst-case parameters. In particular, the temperature is critical. With high-energy magnets, Br and Hc both decrease when the temperature increases, but more importantly, the knee moves to a lower value of Hm, which means that less current is required to demagnetize the magnet. The maximum current that can flow and its phase angle must also be considered. Normally the current is regulated by the inverter, so the maximum current is tightly controlled. But there may be fault conditions where the current reaches a value much higher than normal. In this motor, the "worst case" condition will be deemed to be a three-phase short-circuit with a magnet temperature of 25EC. The current is equal to

$$I_{d[sc]} = \frac{E_{q1}}{X_d} \tag{2}$$

where E_{q1} is the RMS fundamental EMF per phase, and X_d is the d-axis synchronous reactance. Normally this current is from 2 to5 times the maximum operating current.

Table 1. Geometry parameter of LS- PMA-SYNRM

Parameters	**Values**	**Unit**
Slot Number	36	
Outer Stator	210	mm
Inner Stator	132	mm
Tooth Width	5	mm
Slot Depth	19	mm
Motor Length	180	mm
Stator Lam Length	180	mm
Magnet Length	150	mm
Magnet size	5x2	mm
Air gap	0.4	mm
Turn per coil	20	

Table 1 shows the design parameters of LS-PMA-SynRM of pole, slot, and stack length. The rotor topology of the proposed PMA-SYNRM machines is the proposed 3V-shape magnet arrangement. The arrangement of the PM is regarded as requisite for efficient operation. The 3V layer shapes of the prototype model are simple and easy to mass production. The total weight of the magnet segment and copper winding is almost the same. The cost of the magnet is minimized due to expensive. Table 2 shows the material weight of PMA-SYNRM.

Table 2. Geometry parameter of LS- PMA-SYNRM

Parameter	**LS-PMA-SynRM (kg)**
Stator Lam (Back Iron)	8.26
Stator Lam (Tooth)	5.245
Stator Lamination [Total]	13.5
Armature Winding [Active]	4.138
Armature EWdg [Front]	1.027
Armature EWdg [Rear]	1.027
Armature Winding [Total]	6.193
Rotor Lam (Back Iron)	5.37
IPM Magnet Pole	4.833
Rotor Lamination [Total]	10.74
Magnet	0.5
Total	33.98

Figure 4 shows the simulated machine response when the control action of the stator phase winding occurs short circuit. The simulations were carried out for two bus voltage 220VAC, corresponding to the maximum and minimum voltages, respectively, of a battery pack power supply. The speed used for the simulations was 3000 rpm. This is the maximum speed in the desired operating range and represents a worst-case condition since the voltage difference between the machine's back-emf voltage and the bus voltage is largest under these conditions. Since the back-emf voltage is proportional to rotor speed, the post-fault currents disappear entirely when the speed drops to the point that the phase-leg diodes never become forward biased following fault initiation.

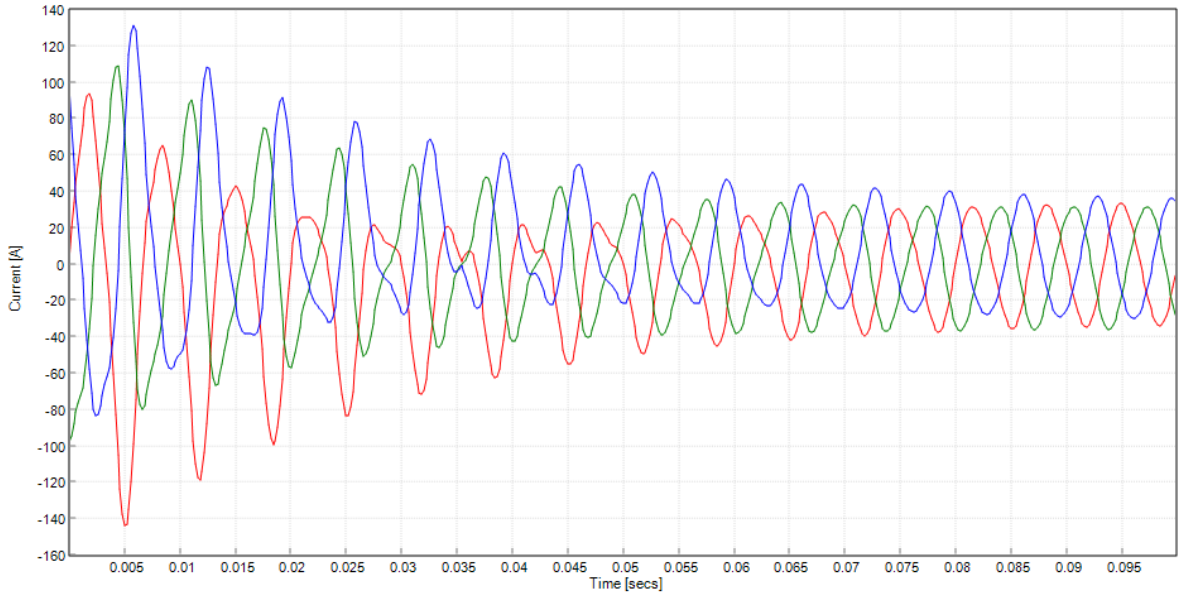

Figure 4 Short circuit current

The peak values of the fault current and torque change little when the rotor speed is changed from 3000 rpm to 2000 rpm. This is due to the fact that the back-emf and the machine reactances are all proportional to rotor speed (i.e., frequency), so that the resulting current associated with their ratio (i.e., E/X) is quite insensitive to speed. It is only at low speeds when the resistance effects become dominant that the currents and torque become increasingly speed-sensitive.

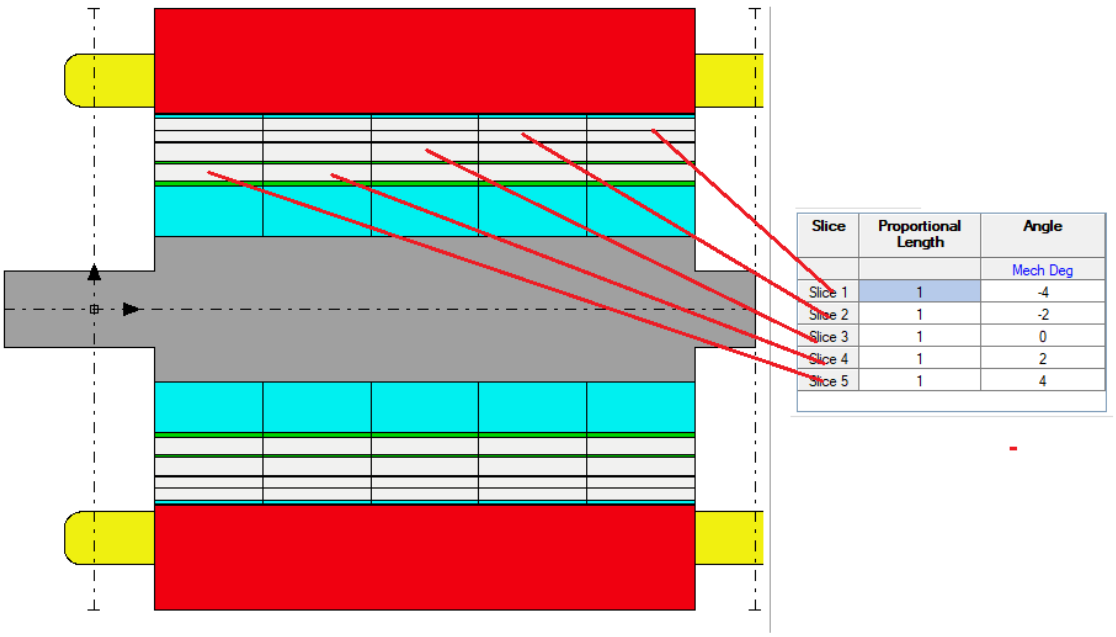

Figure 5 Slice Skewing Rotors

DEMAGNTIZATION ANALYSIS

The proposed LS-PMA-SYNRM machines are designed and analyzed with skewing and nonskewing rotors. The total torque and efficiency are important performance for those motors which were also compared in two models. The demagnetization areas are implemented in the below plotters. Fig. 6 shows the magnetic field distribution of two magnets magnetized in place (in the rotor core) at input currents of 120A. As the input current becomes larger the portion of the magnets near the bridge, which is least magnetized, becomes more magnetized. Where magnetization is low the magnetization is insufficient.

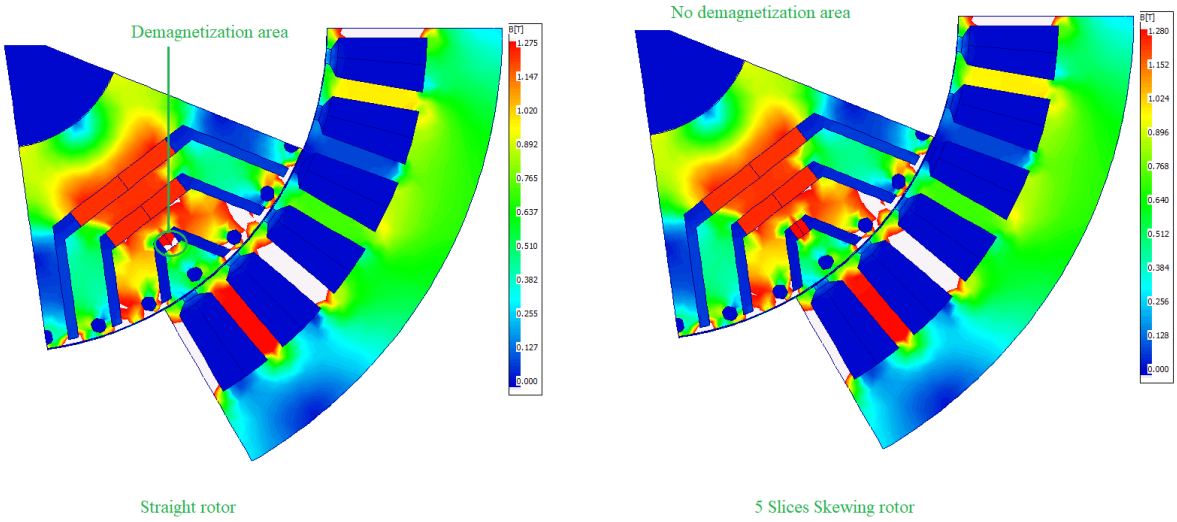

Figure 6. Demagnetization area of Straight Rotor and Slice Skewing Rotors at 80^0C.

Since demagnetization characteristics after magnetization also depend on temperature, a characteristic table was prepared verse several different temperatures where the temperature is for after magnetization from an applied magnetic field. This table was created for the applied magnetic field, temperature, and demagnetization characteristics. When used as magnet material after magnetization, a table of temperature – demagnetization characteristics verse applied magnetic field at the time of magnetization is referenced. Since the applied magnetic field is not uniform inside the magnet, the demagnetization characteristics vary in the magnet.

The back-EMFs at rated speed of the two investigated machines are shown in Figure 7. It can be found that the THD of the Back EMF of the Skewing design is 2.2% less than that of the straight design of 20%. Meanwhile, it shows that the LS-PMA-SynRM motor exhibits better sinusoidal back-EMF than the conventional machine. The cogging torque waveforms are illustrated in below table.

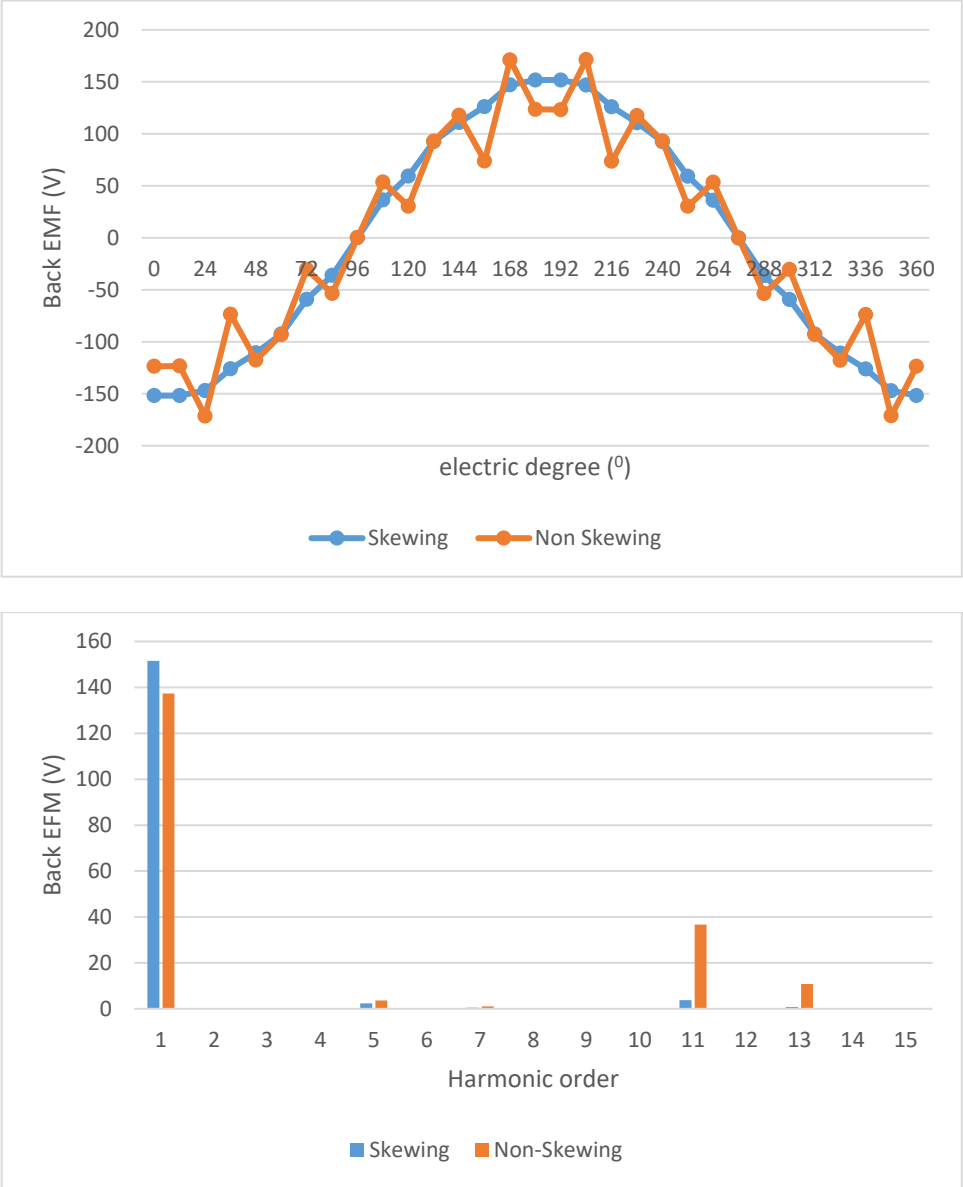

Figure 7. Back EMF and Harmonic comparison of Slice Skewing and Non-Slewing Rotors

The summarized data of the two models are shown in Table 3, which include average torque, torque ripple. The power, total losses, cogging torque, and efficiency under the maximized constant torque control method. The total iron losses consist of core loss and magnet eddy-current loss. The total iron loss of the 5 slices skewing magnets is the lowest. Therefore, model 3 V layer magnets is selected as the prototype machine.

Table 3. Efficiency comparison of LS-PMA-SynRM

LS-PMa-SynRM Parameter	**Straight Slot**	**Skewing Slots**	**Unit**
Shaft Torque	53.67	55.667	Nm
Input Power	9123.3	9273.3	Watts
Output Power	8644.1	8744.1	Watts
Total Losses	519.5	529.15	Watts

System Efficiency	93.24	94.68	%
Armature DC Copper Loss	340	340	Watts
Magnet Loss	178.8	168	Watts
Stator iron Loss	10.33	10.33	Watts
Phase Terminal Voltage	289.1	289.1	Volts
Harmonic Distortion Line-Line Terminal Voltage	4.89	3.089	Volts
Harmonic Distortion Phase Terminal Voltage	13.7	11.27	%
Back EMF Line-Line Voltage	111	114	%

The electromagnetic torque of an PMA-SYNRM machine is formed from two components of magnetic torque and reluctance torque. The PM component is produced based on the interaction between the air-gap magnetic field and armature reaction magnetic field and the reluctance component is instead on asymmetry between the PMA-SYNRM machines magnetic circuit of d-axis and q-axis. The electromanetic torque can then be defined as:

$$T\_em = \frac{3.p}{2}\ [\lambda_{pm}.i_d + (L_d - L_q).i_d.i_q] \quad (3)$$

The λpm depends on magnet sizes, the q-axis inductance and d-axis inductance for PMA-SYNRM machines are calculated based on rotor magnet barrier and magnet pole U shape.

where λ_{PM} is the flux linkage generated by PM field and λ_d is the d-axis flux linkage generated by armature reaction field between rotor and stator. The FEA-calculated d- and q-axis inductances are shown in Figure 3. The DC link voltage of the power inverter to the PM machine is limited by the maximum bus voltage of batteries. The angular speed of the rotor is limited by the amplitude of the phase voltage. Dynamic torque of reluctance and permanent magnetic parts are shown in figure 3.

The peak torque and power versus speed characteristics of 3V shape LS_PMA-SYNRM machine have been verified at 1500 rpm. With the increase of phase current density up to 5 A/mm2, the average torque is 52 Nm. The torque and power performance. Maximum efficiency is 94%. Total losses of iron cores, copper windings have been applied to thermal simulation and temperature results as below table. The temperature distribution of stator, rotor, winding, and magnet was calculated in figure 6. The maximum temperature of winding is 90.7ºC much lower than isolation class H (180^0). The temperature of the magnet is 88 ^{0}C and the detail values of other parts are listed in table 2.

Table 4. The temperature of LS- PMA-SYNRM

No	**Component**	**LS- PMA-SYNRM T (^{0}C)**
1	T [Ambient]	40
2	T [Housing - Active]	78.717
3	T [Stator Lam (back iron)]	84.833
4	T [Stator Surface]	88.403
5	T [Rotor Surface]	88.65
6	T [Airgap Banding]	88.651
7	T [Magnet]	88.197
8	T [Airgap Banding]	88.651
9	T [Rotor Lamination]	87.674
10	T [Shaft - Center]	87.375
13	T [Active Winding Minimum]	87.352

LS-PMA-SynRM temperature of rotor parts are cooler than the temperature of induction motor in table 3 and stator and winding are similar to LS-PMa-SynRMs.

.Conclusions

This paper has analyzed and compared the demagnetization of three multi-layered LS_PMA-SYNRM machines for industrial and traction applications. The 3V shape with 5 slice skewing has the lowest volume of magnets and high torque and power density. Under short circuit conditions, the 3V shape skewing slot-LS-PMA-SYNRM machine has a lower demagnetization level in comparison with the straight design. To verify the proposed design, back EMF and demagnetization performances have been evaluated with limit temperature rises. The back EMF has been analyzed based on the FEA modeling to verify maximum speed. The thermal simulation was implemented to validate overheat capacity.

Acknowledgments. This research was supported Institute for Control Engineering and Automation- ICEA) for High Processing Speed Computer and CAD software to run the analytical program in MATLAB coupling to CAD, FEMM in this study.

REFERENCES

Hyunwoo Kim; Yeji Park;Seung-Taek Oh;Hyungkwan Jang;Dong-Hoon Jung;Ik Sang Jang;Ju Lee, *"Study on Analysis Method of Asymmetric Permanent Magnet Assistance Synchronous Reluctance Motor Considering Magnetic Neutral Plane Shift"* IEEE Transactions on Applied Superconductivity Year: 2020 | Volume: 30, Issue: 4 | Journal Article | Publisher: IEEE

Cheng Gong;Fang Deng, *"Design and Optimization of a Low-Torque-Ripple High-Torque-Density Vernier Machine Using Ferrite Magnets for Low-Speed Direct-Drive Applications"* 2021 IEEE International Electric Machines & Drives Conference (IEMDC), Year: 2021 | Conference Paper | Publisher: IEEE.

B. Ozpineci, "Oak Ridge National Laboratory annual progress report for the electric drive technologies program," Oak Ridge Nat. Lab., Oak Ridge, TN, USA, Tech. Rep. ORNL/SR-2016/640, Oct. 2016.

M. Taniguchi et al., "Development of new hybrid transaxle for compactclass vehicles," SAE Tech. Paper 2016-01-1163, 2016, doi: 10.4271/ 2016-01-1163.

T. Huynh and M.-F. Hsieh, "Comparative study of PM-assisted SynRM and PMA-SYNRMSM on constant power speed range for EV applications," IEEE Trans. Magn., vol. 53, no. 11, Nov. 2017, Art. no. 8211006.

X. Chen, J. Wang, B. Sen, P. Lazari, and T. Sun, "A high-fidelity and computationally efficient model for interior permanent-magnet machines considering the magnetic saturation, spatial harmonics, and iron loss effect," IEEE Trans. Ind. Electron., vol. 62, no. 7, pp. 4044–4055, Jul. 2015

Shushu Zhu , Weifang Chen, Mingqiu Xie, Chuang Liu, and Kai Wang," Electromagnetic Performance Comparison of Multi-Layered Interior Permanent Magnet Machines for EV Traction Applications. IEEE TRANSACTIONS ON MAGNETICS (2020),

Y. Nie, I. P. Brown, and D. C. Ludois, "Deadbeat-direct torque and flux control for wound field synchronous machines," IEEE Trans. Ind. Electron., vol. 65, no. 3, pp. 2069-2079, Mar. 2018.

A. Wang, Y. Jia, and W. L. Soong, "Comparison of five topologies for an interior permanent-magnet machine for a hybrid electric vehicle," IEEE Trans. Magn., vol. 47, no 10, pp. 3606-3609, Oct. 2011.

Bui Minh Dinh is a Lecturer and researcher at Hanoi University of Science and Technology in Vietnam. He received a Ph.D. in Electric Motor Design and Manufacture in 2014 at the Technical University of Berlin, Germany, Among his research interests there are high-speed motor design and manufacture related to industrial products such as SRM, IPM, and IM motors. He has managed Viettel R&D for IDME design and Electromagnetic Advisor for Hanoi Electromechanic Manufacturer. Since 2019 he has been a technical advisor for several Electrical Vehicle Companies in Vietnam Such as M1 Viettel, Selex Motor Abico, and Vinfast